

# SMOOTHED ANOVA WITH SPATIAL EFFECTS AS A COMPETITOR TO MCAR IN MULTIVARIATE SPATIAL SMOOTHING

BY YUFEN ZHANG JAMES S. HODGES AND SUDIPTO BANERJEE\*

**1. Introduction.** Statistical modelling and analysis of spatially referenced data receive considerable interest due to the increasing availability of geographical information systems (GIS) and spatial databases. For data aggregated over geographic regions such as counties, census tracts or ZIP codes (often called *areal* data), with individual identifiers and precise locations removed, inferential objectives focus on models for spatial clustering and variation. Such models are often used in epidemiology and public health to understand geographical patterns in disease incidence and morbidity. Recent reviews of methods for such data include Lawson et al. (1999), Elliott et al. (2000), Waller & Gotway (2004) and Rue & Held (2004). Traditionally such data have been modelled using conditionally specified probability models that shrink or smooth spatial effects by borrowing strength from neighboring regions. Perhaps the most pervasive model is the conditionally autoregressive (CAR) family pioneered by Besag (1974), which has been widely investigated and applied to spatial epidemiological data (Wakefield,

---

\*Yufen Zhang is a senior biostatistician in Novartis Pharmaceuticals, East Hanover, NJ 07936, USA, James S. Hodges and Sudipto Banerjee are Associate Professors in the Division of Biostatistics, School of Public Health, University of Minnesota, Minneapolis, MN, 55455. The work of the third author was supported in part by NIH grant 1-R01-CA95995.

2007, gives an excellent review). Recently the CAR has been extended to multivariate responses, building on multivariate conditional autoregressive (MCAR) models described by Mardia (1988). Gelfand & Vonatsou (2003) and Carlin & Banerjee (2003) discussed their use in hierarchical models, while Kim, Sun & Tsutakawa (2001) presented a different “twofold CAR” model for counts of two diseases in each areal unit. Other extensions allowing flexible modelling of cross-correlations include Sain & Cressie (2002), Jin, Carlin & Banerjee (2005) and Jin, Banerjee & Carlin (2007). The MCAR can be viewed as a conditionally specified probability model for interactions between space and an attribute of interest. For instance, in disease mapping interest often lies in modelling geographical patterns in disease rates or counts of several diseases. The MCAR acknowledges dependence between the diseases as well as dependence across space. However, practical difficulties arise from MCAR’s elaborate dependence structure: most interaction effects will be weakly identified by the data, so the dependence structure is poorly identified. In hierarchical models (e.g., Gelfand & Vonatsou, 2003; Jin et al., 2005, 2007), strong prior distributions may improve identifiability, but this is not uncontroversial as inferences are sensitive to the prior and perhaps unreliable without genuine prior information. This article proposes a much simpler and more interpretable alternative to the MCAR, modelling multivariate spatial effects using smoothed analysis of variance (SANOVA) as developed by Hodges, Cui, Sargent & Carlin (2007), henceforth HCSC. Unlike an ANOVA that is used to identify some interaction effects to retain and others to remove, SANOVA mostly retains effects that are large, mostly removes those that are small, and partially retains middling effects.

(Loosely speaking, “large”, “middling”, and “small” describe the size of the unsmoothed effects compared to their standard errors.) To accommodate rich dependence structures, MCAR introduces weakly identifiable parameters that complicate estimation. SANOVA, on the other hand, focuses instead on smoothing interactions to yield more stable and reliable results. Our intended contribution is to show how SANOVA can solve the multiple disease mapping problem while avoiding the dauntingly complex covariance structures imposed by MCAR and its generalizations. We demonstrate that SANOVA produces inference that is largely indistinguishable from MCAR, yet SANOVA is simpler, more explicit, easier to put priors on and easier to estimate. The rest of the article is as follows. Section 2 reviews SANOVA and MCAR, identifying SANOVA as a special case of MCAR. Section 3 is a “tournament” of simulation experiments comparing SANOVA with MCAR for normal and Poisson data, while Section 4 analyzes data describing the number of deaths from lung, larynx and esophagus cancer in Minnesota between 1990 and 2000. A summary and discussion of future research in Section 5 concludes the paper. Zhang et al. (2009) (Appendices) gives computational and technical details.

## 2. The Competitors.

### 2.1. *Smoothing spatial effects using SANOVA.*

2.1.1. *SANOVA for balanced, single-error-term models (HCSC 2007).* Consider a balanced, single-error-term analysis of variance, with  $M_1$  degrees of freedom for main effects and  $M_2$  degrees of freedom for interactions. Specify this ANOVA as a linear model: let  $A_1$  denote columns in the design matrix

for main effects, and  $A_2$  denote columns in the design matrix for interactions. Assume the design has  $c$  cells and  $n$  observations per cell, giving  $cn$  observations in total. To simplify later calculations, normalize the columns of  $A_1$  and  $A_2$  so  $A_1'A_1 = I_{M_1}$  and  $A_2'A_2 = I_{M_2}$ . (Note: HCSC normalized columns differently, fixing  $A_1'A_1 = cnI_{M_1}$  and  $A_2'A_2 = cnI_{M_2}$ .) Then write the ANOVA as:

$$(1) \quad \mathbf{y} = [A_1|A_2] \begin{bmatrix} \boldsymbol{\Theta}_1 \\ \boldsymbol{\Theta}_2 \end{bmatrix} + \boldsymbol{\epsilon} = A_1\boldsymbol{\Theta}_1 + A_2\boldsymbol{\Theta}_2 + \boldsymbol{\epsilon}$$

where  $\boldsymbol{\epsilon} \sim N(0, \frac{1}{\eta_0}I)$  with  $\eta_0$  being a precision,  $\mathbf{y}$  is  $cn \times 1$ ,  $A_1$  is  $cn \times M_1$ ,  $A_2$  is  $cn \times M_2$ ,  $\boldsymbol{\Theta}_1$  is  $M_1 \times 1$ ,  $\boldsymbol{\Theta}_2$  is  $M_2 \times 1$ , and  $\boldsymbol{\epsilon}$  is  $cn \times 1$ . This ANOVA is smoothed by further modeling  $\boldsymbol{\Theta}$ . HCSC emphasized smoothing interactions, although main effects can be smoothed by exactly the same means. Following HCSC, we add constraints (or a prior) on  $\boldsymbol{\Theta}_2$  as  $\theta_{M_1+j} \sim N(0, 1/\eta_j)$  for  $j = 1, \dots, M_2$ , written as:

$$(2) \quad \mathbf{0}_{M_2} = [0_{M_2 \times M_1} | I_{M_2}] \begin{bmatrix} \boldsymbol{\Theta}_1 \\ \boldsymbol{\Theta}_2 \end{bmatrix} + \boldsymbol{\delta}$$

where  $\boldsymbol{\delta} \sim N(0, \text{diag}(\frac{1}{\eta_j}))$ , in the manner of Lee & Nelder (1996) and Hodges (1998). Combining (1) and (2), express this hierarchical model as a linear model:

$$(3) \quad \begin{bmatrix} \mathbf{y} \\ \mathbf{0}_{M_2} \end{bmatrix} = \begin{bmatrix} A_1 & A_2 \\ 0_{M_2 \times M_1} & I_{M_2} \end{bmatrix} \begin{bmatrix} \boldsymbol{\Theta}_1 \\ \boldsymbol{\Theta}_2 \end{bmatrix} + \begin{bmatrix} \boldsymbol{\epsilon} \\ \boldsymbol{\delta} \end{bmatrix}.$$

More compactly, write:

$$(4) \quad \mathbf{Y} = X\boldsymbol{\Theta} + \mathbf{e}$$

where  $\mathbf{Y}$  has dimension  $(cn + M_2) \times 1$  and  $\mathbf{e}$ 's covariance  $\Gamma$  is block diagonal with blocks  $\Gamma_1 = \frac{1}{\eta_0} I_{cn}$  for the data cases (rows of  $X$  corresponding to the observation  $\mathbf{y}$ ) and  $\Gamma_2 = \text{diag}(1/\eta_1, \dots, 1/\eta_{M_2})$  for the constraint cases (rows of  $X$  with error term  $\boldsymbol{\delta}$ ). For convenience, define the matrix  $X_D = [A_1|A_2]$ , the data-case part of  $X$ . This development can be done using the mixed linear model (MLM) formulation traditionally written as  $\mathbf{y} = X\boldsymbol{\beta} + Z\mathbf{u} + \boldsymbol{\epsilon}$ , where our (1) supplies this equation and  $\mathbf{u} = \boldsymbol{\Theta}_2 \sim N(\mathbf{0}, \Gamma_2)$ . The development to follow can also be done using the MLM formulation at the price of slightly greater complexity, so we omit it. HCSC developed SANOVA for exchangeable priors on groups formed from components of  $\boldsymbol{\Theta}_2$ . The next section develops the extension to spatial smoothing.

2.1.2. *What is CAR?*. Suppose a map has  $N$  regions, each with an unknown quantity of interest  $\phi_i$ ,  $i = 1, \dots, N$ . A conditionally autoregressive (CAR) model specifies the full conditional distribution of each  $\phi_i$  as

$$(5) \quad \phi_i \mid \phi_j, j \neq i, \sim N\left(\frac{\alpha}{m_i} \sum_{i \sim j} \phi_j, \frac{1}{\tau m_i}\right), \quad i, j = 1, \dots, N,$$

where  $i \sim j$  denotes that region  $j$  is a *neighbor* of region  $i$  (typically defined as spatially adjacent), and  $m_i$  is the number of region  $i$ 's neighbors. Equation (5) reduces to the well-known intrinsic conditionally autoregressive (ICAR) model (Besag et al., 1991) if  $\alpha = 1$  or an independence model if  $\alpha = 0$ . The ICAR model induces ‘‘local’’ smoothing by borrowing strength from neighbors, while the independence model assumes spatial independence and induces ‘‘global’’ smoothing. The CAR prior’s smoothing parameter  $\alpha$  also controls the strength of spatial dependence among regions, though it has long been appreciated that a fairly large  $\alpha$  may be required to induce large

spatial correlation; see Wall (2004) for recent discussion and examples. It is well-known (e.g., Besag, 1974) that the conditional specifications in (5) lead to a valid joint distribution for  $\boldsymbol{\phi} = (\phi_1, \dots, \phi_N)'$  expressed in terms of the map's neighborhood structure. If  $Q$  is an  $N \times N$  matrix such that  $Q_{ii} = m_i$ ,  $Q_{ij} = -\alpha$  whenever  $i \sim j$  and  $Q_{ij} = 0$  otherwise, then the intrinsic CAR model (Besag et al 1991) has density:

$$(6) \quad p(\boldsymbol{\phi}|\tau) \sim \tau^{\frac{N^*}{2}} \exp\left(-\frac{\tau}{2}\boldsymbol{\phi}'Q\boldsymbol{\phi}\right), \text{ with } N^* = \begin{cases} N, & \text{if } \alpha \in (0, 1) \\ N - G, & \text{if } \alpha = 1 \end{cases}.$$

In (6),  $\tau$  is the spatial precision parameter,  $\tau Q$  is the precision matrix in this multivariate normal distribution and  $G$  is the number of ‘‘islands’’ (disconnected parts) in the spatial map (Hodges et al 2003). When  $\alpha \in (0, 1)$ , (6) is a proper multivariate normal distribution. When  $\alpha = 1$ ,  $Q$  is singular with  $Q\mathbf{1} = \mathbf{0}$ ;  $Q$  has rank  $N - G$  in a map with  $G$  islands, therefore the exponent on  $\tau$  becomes  $(N - G)/2$ . In hierarchical models, the CAR model is usually used as a prior on spatial random effects. For instance, let  $Y_i$  be the observed number of cases of a disease in region  $i$ ,  $i = 1, \dots, N$ , and  $E_i$  be the expected number of cases in region  $i$ . Here the  $Y_i$  are treated as random variables, while the  $E_i$  are treated as fixed and known, often simply proportional to the number of persons at risk in region  $i$ . For rare diseases, a Poisson approximation to a binomial sampling distribution for disease counts is often used, so a commonly used likelihood for mapping a single disease is

$$(7) \quad Y_i \stackrel{ind}{\sim} Poisson(E_i e^{\mu_i}), \quad i = 1, \dots, N,$$

where  $\mu_i = \mathbf{x}'_i \boldsymbol{\beta} + \phi_i$ . The  $\mathbf{x}_i$  are explanatory, region-specific regressors with coefficients  $\boldsymbol{\beta}$  and the parameter  $\mu_i$  is the log-relative risk describing departures of observed from expected counts, that is, from  $E_i$ . The hierarchy's next

level is specified by assigning the CAR distribution to  $\phi$  and a hyper-prior to the spatial precision parameter  $\tau$ . In the hierarchical setup, the improper ICAR with  $\alpha = 1$  gives proper posterior distributions for spatial effects. In practice, Markov Chain Monte Carlo (MCMC) algorithms are designed for estimating posteriors from such models and the appropriate number of linear constraints on the  $\phi$  suffices to ensure sampling from proper posterior distributions (Banerjee, Carlin & Gelfand, 2004, pp 163–164, gives details).

2.1.3. *How does CAR fit into SANOVA?* To use CAR in SANOVA, the key is re-expressing the improper CAR, i.e., (6) with  $\alpha = 1$ . Let  $Q$  have spectral decomposition  $Q = VDV'$ , where  $V$  is an orthogonal matrix with columns containing  $Q$ 's eigenvectors and  $D$  is diagonal with non-negative diagonal entries.  $D$  has  $G$  zero diagonal entries, one of which corresponds to the eigenvector  $\frac{1}{\sqrt{N}}\mathbf{1}_N$ , by convention the  $N^{\text{th}}$  (right-most) column in  $V$ . Define a new parameter  $\Theta = V'\phi$ , so  $\Theta$  has dimension  $N$  and precision matrix  $\tau D$ . Giving an  $N$ -vector  $\Theta$  a normal prior with mean zero and precision  $\tau D$  is equivalent to giving  $\phi = V\Theta$  a CAR prior with precision  $\tau Q$ .  $\Theta$  consists of  $\Theta_N = \frac{1}{\sqrt{N}}\mathbf{1}'_N\phi = \sqrt{N}\bar{\phi}$ , the scaled average of the  $\phi_i$ , along with  $N - 1$  contrasts in  $\phi$ , which are orthogonal to  $\frac{1}{\sqrt{N}}\mathbf{1}_N$  by construction. Thus the CAR prior is informative (has positive precision) only for contrasts in  $\phi$ , while putting zero precision on  $\Theta_{GM} = \Theta_N = \frac{1}{\sqrt{N}}\mathbf{1}'_N\phi$ , the overall level, and on  $G - 1$  orthogonal contrasts in the levels of the  $G$  islands. In other words, the CAR model can be thought of as a prior distribution on the contrasts rather than individual effects (hence the need for the sum-to-zero constraint). A related result, discussed in Besag et al. (1995), shows the CAR to be a member of a family of “pairwise difference” priors. This

reparameterization allows the CAR model to fit into the ANOVA framework, with  $\Theta_{GM}$  corresponding to the ANOVA's grand mean and the rest of  $\Theta$ ,  $\Theta_{Reg}$ , corresponding to  $V^{(-)'}\phi$ , where  $V^{(-)}$  is  $V$  excluding the column  $\frac{1}{\sqrt{N}}\mathbf{1}_N$ , consisting of  $N - 1$  orthogonal contrasts among the  $N$  regions and giving the  $N - 1$  degrees of freedom in the usual ANOVA:

$$\begin{aligned}\phi &= \begin{bmatrix} \phi_1, \phi_2, \dots, \phi_N \end{bmatrix}' \\ &= V\Theta \\ &= \begin{bmatrix} V^{(-)} & \frac{1}{\sqrt{N}}\mathbf{1}_N \end{bmatrix} \begin{bmatrix} \Theta_{Reg} \\ \Theta_{GM} \end{bmatrix}.\end{aligned}$$

Giving  $\phi$  a CAR prior is equivalent to giving  $\Theta$  a  $N(\mathbf{0}, \tau D)$  prior; the latter are the ‘‘constraint cases’’ in HCSC's SANOVA structure. The precision  $D_{NN} = 0$  for the overall level is equivalent to a flat prior on  $\Theta_{GM}$ , though  $\Theta_{GM}$  could alternatively have a normal prior with mean zero and finite variance. If  $G > 1$ , the CAR prior also puts zero precision on  $G - 1$  contrasts in  $\phi$ , which are contrasts in the levels of the  $G$  islands (Hodges et al 2003).

## 2.2. SANOVA as a competitor to MCAR.

2.2.1. *Multivariate conditionally autoregressive (MCAR) models.* With multiple diseases, we have unknown  $\phi_{ij}$  corresponding to region  $i$  and disease  $j$ , where  $i = 1, \dots, N$  and  $j = 1, \dots, n$ . Letting  $\Omega$  be a common precision matrix (i.e., inverse of the covariance matrix) representing correlations between the diseases in a given region, MCAR distributions arise through conditional specifications for  $\phi_i = (\phi_{i1}, \dots, \phi_{in})'$ :

$$(8) \quad \phi_i | \{\phi_{i'}\}_{i' \neq i} \sim MVN \left( \frac{\alpha}{m_i} \sum_{i' \sim i} \phi_{i'}, \frac{1}{m_i} \Omega^{-1} \right).$$

These conditional distributions yield a joint distribution for  $\phi = (\phi_1', \dots, \phi_N)'$ :

$$(9) \quad f(\phi|\Omega) \propto \|\Omega\|^{\frac{N-G}{2}} \exp\left(-\frac{1}{2}\phi'(Q \otimes \Omega)\phi\right),$$

where  $Q$  is defined as in Section 2.1.2 and again (9) is an improper density when  $\alpha = 1$ . However, as for the univariate CAR, this yields proper posteriors in conjunction with a proper likelihood. The specification above is a “separable” dispersion structure, i.e., the covariances between the diseases are invariant across regions. This may seem restrictive, but relaxing this restriction gives even more complex dispersion structures (see Jin, Banerjee & Carlin, 2007 and references therein). As mentioned earlier, our focus is to retain the model’s simplicity without compromising the primary inferential goals. We propose to do this using SANOVA and will compare it with the separable MCAR only.

2.2.2. *SANOVA with Minnesota counties as one factor.* We now describe the SANOVA model using the Minnesota 3-cancer dataset. Consider the Minnesota map with  $N = 87$  counties, and suppose each county has counts for  $n = 3$  cancers. County  $i$  has an  $n$ -vector of parameters describing the  $n$  cancers,  $\phi_i = (\phi_{i1}, \phi_{i2}, \dots, \phi_{in})'$ ; define the  $Nn$  vector  $\phi$  as  $\phi = (\phi_1', \phi_2', \dots, \phi_N)'$ . For now, we are vague about the specific interpretation of  $\phi_{ij}$ ; the following description applies to any kind of data. Assume the  $N \times N$  matrix  $Q$  describes neighbor pairs among counties as before. The SANOVA model for this problem is a 2-way ANOVA with factors cancer (“CA”,  $n$  levels) and county (“CO”,  $N$  levels) and no replication. As in section 2.1.1, we model  $\phi$  with a saturated linear model and put the grand mean and the main effects in their traditional positions as in ANOVA

(matrix dimensions and definitions appear below the equation):

$$\phi = [\phi_1', \phi_2', \dots, \phi_N']' = [A_1 | A_2] \Theta = \quad (10)$$

$$\left[ \underbrace{\frac{1}{\sqrt{Nn}} \mathbf{1}_{Nn}} \quad \underbrace{\frac{1}{\sqrt{N}} \mathbf{1}_N \otimes H_{CA}} \quad \underbrace{V^{(-)} \otimes \frac{1}{\sqrt{n}} \mathbf{1}_n} \quad \underbrace{V^{(-)} \otimes H_{CA}^{(1)} \dots V^{(-)} \otimes H_{CA}^{(n-1)}} \right] \begin{bmatrix} \Theta_{GM} \\ \Theta_{CA} \\ \Theta_{CO} \\ \Theta_{CO \times CA} \end{bmatrix}$$

	Cancer	County	Cancer×County
Grand mean	main effect	main effect	interaction
$Nn \times 1$	$Nn \times (n-1)$	$Nn \times (N-1)$	$Nn \times (N-1)(n-1)$

where  $H_{CA}$  is an  $n \times (n-1)$  matrix whose columns are contrasts among cancers, so  $\mathbf{1}'_n H_{CA} = \mathbf{0}'_{n-1}$ , and  $H'_{CA} H_{CA} = I_{n-1}$ ;  $H_{CA}^{(j)}$  is the  $j^{\text{th}}$  column of  $H_{CA}$ ; and  $V^{(-)}$  is  $V$  without its  $N^{\text{th}}$  column  $\frac{1}{\sqrt{N}} \mathbf{1}_N$ , so it has  $N-1$  columns, each a contrast among counties, i.e.,  $\mathbf{1}'_N V^{(-)} = \mathbf{0}'_{N-1}$ , and  $V^{(-)'} V^{(-)} = I_{N-1}$ . The column labelled “Grand mean” corresponds to the ANOVA’s grand mean and has parameter  $\Theta_{GM}$ ; the other blocks of columns labeled as main effects and interactions correspond to the analogous ANOVA effects and to their respective parameters  $\Theta_{CA}$ ,  $\Theta_{CO}$ ,  $\Theta_{CO \times CA}$ . Defining prior distributions on  $\Theta$  completes the SANOVA specification. We put independent flat priors (normal with large variance) on  $\Theta_{GM}$  and  $\Theta_{CA}$ , which are, therefore, not smoothed. This is equivalent to putting a flat prior on each of the  $n$  cancer-specific means. To specify the smoothing priors, define  $H_{CA}^{(0)} = \frac{1}{\sqrt{n}} \mathbf{1}_n$ . Let the county main effect parameter  $\Theta_{CO}$  have prior  $\Theta_{CO} \sim N_{N-1}(\mathbf{0}, \tau_0 D^{(-)})$ , where  $D^{(-)}$  corresponds to  $V^{(-)}$  i.e.,  $D$  without its  $N^{\text{th}}$  row and column,  $\tau_0 > 0$  is unknown and  $\tau_0 D^{(-)}$  is a precision matrix.

Similarly, let the  $j^{\text{th}}$  group of columns in the cancer-by-county interaction,  $V^{(-)} \otimes H_{CA}^{(j)}$ , have prior  $\Theta_{CO \times CA}^{(j)} \sim N_{N-1}(\mathbf{0}, \tau_j D^{(-)})$ , for  $\tau_j > 0$  unknown. Each of the priors on  $\Theta_{CO}$  and the  $\Theta_{CO \times CA}^{(j)}$  is a CAR prior; the overall level of each CAR, with prior precision zero, has been included in the grand mean and cancer main effects.

To compare this to the MCAR model, use SANOVA's priors on  $\Theta$  to produce a marginal prior for  $\phi$  comparable to the MCAR's prior on  $\phi$  (section 2.2.1); in other words, integrate  $\Theta_{CO}$  and  $\Theta_{CO \times CA}$  out of the foregoing setup. *A priori*,

$$(11) \quad \left[ K \begin{pmatrix} \Theta_{CO} \\ \Theta_{CO \times CA}^{(1)} \\ \vdots \\ \Theta_{CO \times CA}^{(n-1)} \end{pmatrix} \right]$$

has precision  $Q \otimes (H_A^{(+)} \text{diag}(\tau_j) H_A^{(+)'})$ , where  $K$  is the columns of the design matrix for the county main effects and cancer-by-county interactions—the right-most  $n(N-1)$  columns in equation (10)'s design matrix—and  $H_A^{(+)} = (\frac{1}{\sqrt{n}} \mathbf{1}_n | H_{CA})$  is an orthogonal matrix. Appendix A in Zhang et al. (2009) gives a proof.

2.2.3. *Comparing SANOVA vs MCAR.* Defining  $\phi$  as in sections 2.2.1 and 2.2.2, consider the MCAR prior for  $\phi$ , with within-county precision matrix  $\Omega$ . Let  $\Omega$  have spectral decomposition  $V_\Omega D_\Omega V_\Omega'$ , where  $D_\Omega$  is  $n \times n$  diagonal and  $V_\Omega$  is  $n \times n$  orthogonal. Then the prior precision of  $\phi$  is  $Q \otimes (V_\Omega D_\Omega V_\Omega')$ , where  $Q$  is the known neighbor relations matrix and  $V_\Omega$  and  $D_\Omega$  are unknown. Comparing MCAR to SANOVA, the prior precision matrices for the vector  $\phi$  are as in Figure 1. SANOVA is clearly a special case of MCAR in which  $H_A^{(+)}$  is known. Also, as described so far,  $H_A^{(+)}$  has one

column proportional to  $\mathbf{1}_n$  with the other columns being contrasts, while MCAR avoids this restriction. MCAR is thus more flexible, while SANOVA is simpler, presumably making it better identified and easier to set priors for. MCAR should have its biggest advantage over SANOVA when the “true”  $V_\Omega$  is not like  $H_A^{(+)}$  for any specification of the smoothing precisions  $\tau_j$ . However, because datasets often have modest information about higher-level variances, it may be that using the wrong  $H_A^{(+)}$  usually has little effect on the analysis. In other words, SANOVA’s performance may be relatively stable despite having to specify  $H_A^{(+)}$ , while MCAR may be more sensitive to  $\Omega$ ’s prior.

### 2.3. *Setting priors in MCAR and SANOVA.*

2.3.1. *Priors in SANOVA.* For the case of normal errors, based on equations (1) and (10), setting priors for  $\Theta, \tau_j, \eta_0$  completes a Bayesian specification. Since  $\tau$  and  $\eta_0$  are precision parameters, one possible prior is Gamma; this paper uses a Gamma with mean 1 and variance 10. As mentioned, the grand mean and cancer main effects  $\theta_1, \theta_2, \theta_3$  have flat priors with  $\pi(\theta) \propto 1$ , though they could have proper informative priors. The priors for  $\theta_4, \dots$  are set according to the SANOVA structure as in section 2.2.2. We ran chains drawing in the order  $\theta, \tau$ , and  $\eta_0$  (Appendix B in Zhang et al. (2009) gives details). Hodges et al. (2007) also considered priors on the degrees of freedom in the fitted model, some conditioned so the degrees of freedom in the model’s fit were fixed at a certain degree of smoothness. The present paper emphasizes comparing MCAR and SANOVA, so we do not consider such priors. For the case of Poisson errors, we use a normal prior with mean 0

and variance  $10^6$  for the grand mean and cancer main effects  $\theta_1, \theta_2, \theta_3$ . The other  $\theta_i$ s are given normal CAR priors as discussed in section 2.2.2. For the prior on the smoothing precisions  $\tau_j$ , we use Gamma with mean 1 and variance 10. To reduce high posterior correlations among the  $\theta$ s, we used a transformation during MCMC; Appendix C in Zhang et al. (2009) gives details.

2.3.2. *Priors in MCAR.* MCAR models were fitted in WinBUGS. For the normal-error case, we used this model and parameterization:

$$Y_{ij} \sim N(\mu_{ij}, \frac{1}{\eta_0})$$

$$\mu_{ij} = \beta_j + S_{ij},$$

(12)

$i = 1, \dots, N; j = 1, \dots, n$ , where  $\eta_0$  has a gamma prior with mean 1 and variance 10 as for SANOVA. To satisfy WinBUGS's constraint that  $\sum_i S_{ij} = 0$ , we add cancer-specific intercepts  $\beta_j$ . We give  $\beta_j$  a flat prior and for  $S$ , the spatial random effects, we use an intrinsic multivariate CAR prior. Similarly, in the Poisson case

$$Y_{ij} \sim Poisson(\mu_{ij})$$

$$\log(\mu_{ij}) = \log(E_{ij}) + \beta_j + S_{ij}$$

(13)

where  $E_{ij}$  is an offset. Prior settings for  $\beta_j$  and  $S_{ij}$  are as in the normal case. For MCAR priors, the within-county precision matrix  $\Omega$  needs a prior; a Wishart distribution is an obvious choice. If  $\Omega \sim Wishart(R, \nu)$ , then  $E(\Omega) = \nu R^{-1}$ . We want a "vague" Wishart prior; usually  $\nu = n$  is used but little is known about how to specify  $R$ . Thus, we considered three different

$R$ s, each proportional to the identity matrix. One of these priors sets  $R$ 's diagonal entries to  $R_{ii} = 0.002$ , close to the setting used in an example in the GeoBUGS manual (oral cavity cancer and lung cancer in West Yorkshire). The other two  $R$ s are the identity matrix and 200 times the identity. For the special case  $n = 1$ , where the Wishart reduces to a Gamma, these Wisharts are  $\Gamma(0.5, 0.001)$ ,  $\Gamma(0.5, 0.5)$  and  $\Gamma(0.5, 100)$ , respectively.

**3. Simulation Experiment.** For this simulation experiment, artificial data were simulated from the model used in SANNOVA with a spatial factor, as described in section 2.2.2. Three different types of Bayesian analysis were applied to the simulated data: SANNOVA with the same  $H_A^{(+)}$  used to generate the simulated data (called “SANNOVA correct”); SANNOVA with incorrect  $H_A^{(+)}$ ; and MCAR. SANNOVA correct is a theoretical best possible analysis in that it takes as known things that MCAR estimates, i.e., it uses additional correct information. SANNOVA correct cannot be used in practice, of course, because the true  $H_A^{(+)}$  is not known. MCAR vs SANNOVA with incorrect  $H_A^{(+)}$  is the comparison relevant to practice, and comparing them to SANNOVA correct shows how much each method pays for its “deficiency” relative to SANNOVA correct. Obviously it is not enough to test the SANNOVA model using only data generated from a similar SANNOVA model. To avoid needless computing and facilitate comparisons, instead of generating data from an MCAR model and fitting a SANNOVA model as specified above, we use a trick that is equivalent to this. Section 3.1.2 gives the details.

3.1. *Design of the simulation experiment.* We simulated both normally-distributed and Poisson-distributed data. For both types of data, we consid-

ered two different true sets of smoothing parameters  $\boldsymbol{r} = \boldsymbol{\tau}/\eta_0$  or  $\boldsymbol{\tau}$  (Table 1). For the normal data, we considered  $\boldsymbol{\tau}/\eta_0$ , since this ratio determines smoothing in normal models, and we also considered two error precisions  $\eta_0$  (Table 1).

3.1.1. *Generating the simulated datasets.* To generate data from the SANOVA model, we need to define the true  $H_A^{(+)}$ . Let

$$HA_1 = \begin{pmatrix} 1 & -2 & 0 \\ 1 & 1 & -1 \\ 1 & 1 & 1 \end{pmatrix} \begin{pmatrix} \frac{1}{\sqrt{3}} & 0 & 0 \\ 0 & \frac{1}{\sqrt{6}} & 0 \\ 0 & 0 & \frac{1}{\sqrt{2}} \end{pmatrix}.$$

We used  $HA_1$  as the correct  $H_A^{(+)}$ ; its columns are scaled to have length 1. Given  $V^{(-)}$  and with  $H_A^{(+)}$  known, one draw of  $\Theta$  and  $\epsilon$  produces a draw of  $X_D\Theta + \epsilon$ , therefore a draw of  $\boldsymbol{y}$ . In the simulation, we let the grand mean and main effects, which are not smoothed, have true value 5. Each observation is simulated from a  $3 \times 20$  factorial design, where 3 is the number of cancers and 20 is the number of counties. We used the 20 counties in the right lower corner of Minnesota’s map, with their actual neighbor relations. Thus, the dimension of each artificial dataset is 60. The simulation experiment is a repeated-measures design, in which a “subject”  $s$  in the design is a draw of  $(\boldsymbol{\delta}^{(s)}, \boldsymbol{\gamma}^{(s)})$ , referring to equation (3), where  $\boldsymbol{\delta}_{1-3}^{(s)} = 5$  and  $\boldsymbol{\delta}_{4-60}^{(s)} \sim N_{57}(\mathbf{0}, I_3 \otimes D^{(-)})$  specify  $\Theta$  and  $\boldsymbol{\gamma}^{(s)} \sim N_{60}(\mathbf{0}, I_{60})$  gives  $\epsilon$ . For the normal-errors case, 100 such “subjects” were generated. Given a design cell in the simulation experiment with  $\boldsymbol{\tau} = (a, b, c)$  and  $\eta_0 = d$ , the artificial dataset for subject  $s$  is  $\boldsymbol{y}^{(s)} = X_D \text{diag}(\mathbf{1}'_3, \frac{1}{\sqrt{a}}\mathbf{1}'_{19}, \frac{1}{\sqrt{b}}\mathbf{1}'_{19}, \frac{1}{\sqrt{c}}\mathbf{1}'_{19})\boldsymbol{\delta}^{(s)} + \frac{1}{\sqrt{d}}\boldsymbol{\gamma}^{(s)}$ . All factors of the simulation experiment were applied to each of the 100 “subjects”. For the normally-distributed data, the simulation experiment had these factors: (a) the true  $(\tau_0/\eta_0, \tau_1/\eta_0, \tau_2/\eta_0) : (100, 100, 0.1)$  or  $(0.1, 100, 0.1)$ ; (b)

the true error precision  $\eta_0$ : 1 or 10; and (c) six statistical methods, described below in section 3.1.2. Each design cell described in Table 1 thus had 100 simulated data sets. Similarly, for the Poisson-data experiment, another 100 “subjects” were generated, but now there is no  $\gamma^{(s)}$ . Thus, each “subject”  $s$  is a vector  $\delta^{(s)}$ , where  $\delta^{(s)}$  is as described above. For the design cell with  $\tau = (100, 100, 0.1)$ , the artificial data for subject  $s$  is  $\mathbf{y}^{(s)} \sim \text{Poisson}(\boldsymbol{\mu}^{(s)})$ , where  $\log(\boldsymbol{\mu}^{(s)}) = \log(\mathbf{E}) + X_D \text{diag}(\mathbf{1}'_3, \frac{1}{10}\mathbf{1}'_{19}, \frac{1}{10}\mathbf{1}'_{19}, \frac{1}{\sqrt{0.1}}\mathbf{1}'_{19})\boldsymbol{\delta}^{(s)}$ . In the simulation experiment, we use “internal standardization” of the Minnesota 3-cancer data to supply the expected numbers of cancers  $E_{ij}$ . Among the 20 extracted counties, Hennepin county has the largest average population over 11 years, about 1.1 million; its cancer counts are 5294, 119, 439 for lung, larynx, and esophagus respectively. Faribault county has the smallest average population, 16,501, with cancer counts 110, 7 and 13 respectively. The  $E_{ij}$  have ranges 80 to 5275, 2 to 113 and 7 to 449 for lung, larynx, and esophagus cancer respectively. For the Poisson data, the simulation experiment had these factors: (a) the true  $\tau_0, \tau_1, \tau_2 : (100, 100, 0.1)$  or  $(0.1, 100, 0.1)$ ; and (b) six statistical methods described below in section 3.1.2. Again, each of the two design cells in Table 1 had 100 simulated datasets.

3.1.2. *The six methods (procedures).* For each simulated dataset, we did a Bayesian analysis for each of six different models described in Table 2. The six models are: SANOVA with the correct  $H_A^{(+)}$ ,  $HA_1$ ; SANOVA with a somewhat incorrect  $H_A^{(+)}$ ,  $HA_2$  given below; a variant SANOVA with a very incorrect  $H_A^{(+)}$ ,  $H_{AM}$  given below; MCAR with  $R_{ii} = 0.002$ ; MCAR with  $R_{ii} = 1$ ; and MCAR with  $R_{ii} = 200$  (see section 2.3.2).  $HA_2$  and  $H_{AM}$  are

$$HA_2 = \begin{pmatrix} 1 & 1 & 1 \\ 1 & -2 & 0 \\ 1 & 1 & -1 \end{pmatrix} \begin{pmatrix} \frac{1}{\sqrt{3}} & 0 & 0 \\ 0 & \frac{1}{\sqrt{6}} & 0 \\ 0 & 0 & \frac{1}{\sqrt{2}} \end{pmatrix}, \quad H_{AM} = \begin{pmatrix} 0.56 & -0.64 & -0.52 \\ -0.53 & -0.77 & 0.36 \\ -0.63 & 0.07 & -0.77 \end{pmatrix}.$$

The incorrect  $HA_2$  has the same first column (grand mean) as the correct  $HA_1$ , so it differs from the correct  $HA_1$ , though less than it might. As noted above, we need to see how the SANOVA model performs for data generated from an MCAR model in which  $V_\Omega$  from Figure 1 does not have a column proportional to  $\mathbf{1}_n$ . To do this without needless computing, we used a trick: we used the data generated from a SANOVA model with  $HA_1$  and fit the variant SANOVA mentioned above, in which  $H_A^{(+)}$  is replaced by the orthogonal matrix  $H_{AM}$  with no column proportional to  $\mathbf{1}_n$ , chosen to be very different from  $HA_1$ . For normal errors (Data1 through Data4), this is precisely equivalent to fitting a SANOVA with  $H_A^{(+)} = HA_1$  to data generated from an MCAR model with  $V_\Omega = BHA_1$ , for  $B = HA_1H_{AM}^{-1}$ , i.e.,

$$(14) \quad V_\Omega = \begin{bmatrix} 0.43 & -0.74 & -0.52 \\ -0.13 & -0.63 & 0.77 \\ -0.89 & -0.26 & -0.37 \end{bmatrix}$$

(to 2 decimal places). For Poisson errors (Data5, Data6), the equivalence is no longer precise but the divergence of fitted SANOVA (using  $H_A^{(+)} = H_{AM}$ ) and generated data (using  $H_A^{(+)} = HA_1$ ) is quite similar. Finally, we considered three priors for MCAR because little is known about how to set this prior and we did not want to hobble MCAR with an ill-chosen prior. For the SANOVA and variant SANOVA analyses, we gave  $\tau_j$  a  $\Gamma(0.1, 0.1)$  prior with mean 1 and variance 10 for both the normal data and the Poisson data.

3.2. *Outcome measures.* To compare the six different methods for normal and Poisson data, we consider three criteria. The first is average mean squared error (AMSE). For each of the 60  $(X_D \Theta)_{ij}$ , the mean squared er-

ror is defined as the average squared error over the 100 simulated datasets. AMSE for each design cell in the simulation experiment is defined as the average of mean squared error over the 60  $(X_D \Theta)_{ij}$ . Thus for the design cell labelled DataK in Table 1, define

$$(15) \quad \widehat{AMSE}_K = \frac{1}{L} \sum_{d=1}^L \sum_{i=1}^N \sum_{j=1}^n [(X_D \widehat{\Theta})_{ij}^d - (X_D \Theta)_{ij}^d]^2 / Nn,$$

where  $L = 100, N = 20, n = 3, K = 1, \dots, 4$  for Normal,  $K = 5, 6$  for Poisson,  $\Theta$  is the true value and  $\widehat{\Theta}$  is the posterior median of  $\Theta$ . For each design cell ( $K$ ), the Monte Carlo standard error for AMSE is  $(100)^{-0.5}$  times the standard deviation, across DataK's 100 simulated datasets, of  $\sum_{i=1}^N \sum_{j=1}^n [(X_D \widehat{\Theta})_{ij}^d - (X_D \Theta)_{ij}^d]^2 / Nn$ . The second criterion is the bias of  $X_D \Theta$ . For each of DataK's 100 simulated datasets, first compute posterior medians of  $(X_D \Theta)_{1,1}, \dots, (X_D \Theta)_{20,3}$ , then average each of those posterior medians across the 100 simulated datasets. From this average, subtract the true  $(X_D \Theta)_{ij}$ s to give the estimated bias for each of the 60  $(X_D \Theta)_{ij}$ s. MBIAS is defined as the 2.5<sup>th</sup>, 50<sup>th</sup> and 97.5<sup>th</sup> percentiles of the 60 estimated biases. More explicitly, for design cell DataK, MBIAS is:

$$(16) \quad \widehat{MBIAS}_K = 2.5^{th}, 50^{th}, 97.5^{th} \text{ percentiles of } \left( \frac{1}{L} \sum_{d=1}^L (X_D \widehat{\Theta}^d - X_D \Theta^d) \right).$$

Finally, the coverage rate of Bayesian 95% equal-tailed posterior intervals, "PI rate", is the average coverage rate for the 60 individual  $(X_D \Theta)_{ij}$ s.

**3.3. Markov chain Monte Carlo specifics.** While the MCAR models were implemented in WinBUGS, our SANOVA implementations were coded in R and run on Unix. The different architectures do not permit a fair comparison between the run times of SANOVA and MCAR. However, the SANOVA

models have lower computational complexity than the MCAR models: MCAR demands a spectral decomposition in every iteration, while SANOVA does not. For each of our models, we ran three parallel MCMC chains for 10000 iterations. The CODA package in R ([www.r-project.org](http://www.r-project.org)) was used to diagnose convergence by monitoring mixing using Gelman-Rubin diagnostics and autocorrelations (e.g., Gelman et al., 2003, Section 11.6). Sufficient mixing was seen within 500 iterations for the SANOVA models, while 200 iterations typically revealed the same for the MCAR models; we retained  $8000 \times 3$  samples for the posterior analysis.

3.4. *Results.* Table 3 and Figures 2 and 3 show the simulation experiment's results. Table 3 shows AMSE; for all methods and design cells, the standard Monte Carlo errors of AMSE are small, less than 0.07, 0.005, 0.025 for Data1/Data2, Data3/Data4 and Data5/Data6 respectively. Figure 2 shows MBIAS, where the middle symbols represent the median bias and the line segments represent the 2.5<sup>th</sup> and 97.5<sup>th</sup> percentiles. Figure 3 shows coverage of the 95% posterior intervals. Denote SANOVA with the correct  $H_A^{(+)}$  ( $HA_1$ ) as "SANOVA correct", SANOVA with  $HA_2$  as "SANOVA incorrect", the variant SANOVA with  $H_{AM}$  as "SANOVA variant", MCAR with  $R_{ii} = 0.002$  as "MCAR0.002" and so on.

3.4.1. *As expected, SANOVA with correct  $H_A^{(+)}$  performs best..* For normal data, SANOVA correct has the smallest AMSE for all true  $\eta_0$  and  $\tau$  (Table 3). The advantage is larger in Data1 and Data2 where the error precision  $\eta_0$  is 1, than in Data3 and Data4 where  $\eta_0$  is 10 (i.e., error variation is smaller). For Poisson data, SANOVA correct also has the smallest AMSE.

Considering MBIAS (Figure 2), SANOVA correct has the narrowest MBIAS intervals for all cases. In Figure 3, the posterior coverage for SANOVA correct is nearly nominal. As expected, then, SANOVA correct performs best among the six methods.

3.4.2. *SANOVA with incorrect  $H_{A2}$  and  $H_{AM}$  perform very well.* Table 3 shows that for normal data, both SANOVA incorrect and SANOVA variant have smaller AMSEs than MCAR200 and MCAR0.002, and AMSEs at worst close to MCAR1's. For Poisson data, Table 3 shows that MCAR0.002 and MCAR1 do somewhat better than SANOVA incorrect and variant SANOVA. Considering MBIAS in normal data (Figure 2a), the width of the 95% MBIAS intervals for SANOVA incorrect are the same as or smaller than for all three MCAR procedures. Similarly, SANOVA variant has MBIAS intervals better than MCAR0.002 and MCAR200 and almost as good as MCAR1. Figure 2b for Poisson data shows SANOVA correct, MCAR0.002 and MCAR1 have similar MBIAS intervals. SANOVA variant in Data5 and SANOVA incorrect in Data6 show the worst performance for MBIAS apart from MCAR200, whose MBIAS interval is much the widest. Figure 3a shows that for normal data, interval coverage for SANOVA incorrect and SANOVA variant is very close to nominal. It appears that the specific value of  $H_A^{(+)}$  has little effect on PI coverage rate for the cases considered here. Apart from MCAR200 for Data1/Data2 and MCAR0.002 for Data1 through Data4, which show low coverage, all the other methods have coverage rates greater than 90% for normal data, most close to 95%. For Data3 and Data4, PI rates for MCAR200 reach above 99%. For Poisson data, the PI rates for SANOVA incorrect and SANOVA variant are close

to nominal and better than MCAR0.002 and MCAR200. In particular, all SANOVAs have the closest to nominal coverage rates for both normal and Poisson data, which again shows the stability of SANOVA under different  $H_A^{(+)}$  settings.

3.4.3. *MCAR is sensitive to the prior on  $\Omega$ .* To fairly compare SANOVA and MCAR, we considered MCAR under three different prior settings. For normal data, MCAR1 has the smallest AMSEs and narrowest MBIAS intervals among the MCARs considered, while MCAR0.002 has the largest and widest, respectively. For Poisson data, however, MCAR0.002 has the best AMSE and MBIAS among the MCARs. MCAR200 performs poorly for both Normal and Poisson. The coverage rates in Figure 3 show similar comparisons. These results imply that the prior matters for MCAR: no single prior was always best. By comparison, SANOVA seems more robust, at least for the cases considered.

3.5. *Summary.* As expected, SANOVA correct had the best performance because it uses more correct information. For normal data, SANOVA incorrect and SANOVA variant had similar AMSEs, better than two of the three MCARs for the datasets considered. For Poisson data, SANOVA incorrect and SANOVA variant had AMSEs as good as those of MCAR0.002 and MCAR1 for Data5 and somewhat worse for Data 6, while showing nearly nominal coverage rates in all cases and less tendency to bias than MCAR in most cases. Replacing the  $\Gamma(0.1, 0.1)$  prior for  $\tau$  with  $\Gamma(0.001, 0.001)$  left AMSE and MBIAS almost unchanged and coverage rates a bit worse (data not shown). MCAR, on the other hand, seems more sensitive to the prior

on  $\Omega$ . MCAR0.002 tends to smooth more than MCAR1, more so in normal models where the prior is more influential than in Poisson models. (The latter is true because data give more information about means than variances, and the Poisson model's error variance is the same as its mean, while the normal model's is not.) For the normal data, MCAR0.002's tendency to extra shrinkage appears to make it oversmooth and perform poorly for Data2 and Data4, where the truth is least smooth. For the Poisson data, MCAR0.002 and MCAR1 give results similar to each other and somewhat better than the SANOVAs except for interval coverage. Therefore SANOVA, with stable results under different  $H_A^{(+)}$  and with parameters that are easier to understand and interpret, may be a good competitor to MCAR in multivariate spatial smoothing.

**4. Example: Minnesota 3-cancer data.** Researchers in different fields have illustrated that accounting for spatial correlation could provide insights that would have been overlooked otherwise, while failure to account for spatial association could potentially lead to spurious and sometimes misleading results (see, e.g. Turechek and Madden, 2002; Ramsay et al., 2003; Lichstein et al., 2002). Among the widely investigated diseases are the different types of cancers. We applied SANOVA and MCAR to a cancer-surveillance dataset describing total incidence counts of 3 cancers (lung, larynx, esophagus) in Minnesota's 87 counties for the years 1990 to 2000 inclusive. Minnesota's geography and history make it plausible that disease incidence would show spatial association. Three major North American land forms meet in Minnesota: the Canadian Shield to the north, the Great Plains to the west, and the eastern mixed forest to the southeast. Each of these regions is dis-

tinctive in both its terrain and its predominant economic activity: mining and outdoors tourism in the mountainous north, highly mechanized crop cultivation in the west, and dairy farming in the southeast. The different regions were also settled by somewhat different groups of in-migrants, e.g., disproportionately many Scandinavians in the north. These factors imply spatial association in occupational hazards as well as culture, weather, and access to health care especially in the thinly-populated north, which might be expected to produce spatial association in diseases. With multiple cancers one obvious option is to fit a separate univariate model for each cancer. But diseases may share the same spatially distributed risk factors, or the presence of one disease might encourage or inhibit the presence of another in a region, for example, larynx and esophagus cancer have been shown to be closely related spatially (Baron et al 1993). Thus, we may need to account for dependence among the different cancers while maintaining spatial dependence between sites. Although the dataset has counts broken out by age groups, for the present purpose we ignore age standardization and just consider total counts for each cancer. Age standardization would affect only the expected cancer counts  $E_{ij}$ , while other covariates could be added to either SANOVA or MCAR as unsmoothed fixed effects (i.e., in the  $A_1$  design matrix). Given the population and disease count of each county, we estimated the expected disease count for each cancer in each county using the Poisson model. Denote the  $87 \times 3$  counts as  $y_{1,1}, \dots, y_{87,3}$ ; then the model is

$$(17) \quad \begin{aligned} y_{ij} | \mu_{ij} &\sim \text{Poisson}(\mu_{ij}) \\ \log(\mu_{ij}) &= \log(E_{ij}) + (X_D \Theta)_{ij}, \end{aligned}$$

where  $X_D\Theta$  is the SANOVA structure and  $\Theta$  has priors as in section 2.2.2. For disease  $j$  in county  $i$ ,  $E_{ij} = P_i \frac{\sum_i O_{ij}}{\sum_i P_i}$ , where  $O_{ij}$  is the disease count for county  $i$  and disease  $j$  and  $P_i$  is county  $i$ 's population. For the SANOVA design matrix, we consider  $HA_1$  and  $HA_2$  from the simulation experiment, though now neither is known to be correct. We also consider a variant SANOVA analysis using  $H_A^{(+)}$  estimated from the MCAR1 model, to test the stability of the SANOVA results. Appendix D in Zhang et al. (2009) describes the latter analysis. Figures 4 to 6 show the data and results for MCAR1 and SANOVA with  $HA_1$ . In each Figure, the upper left plot shows the observed  $y_{ij}/E_{ij}$ ; the two lower plots show the posterior median of  $\mu_{ij}/E_{ij}$  for MCAR1 and SANOVA with  $HA_1$ . Lung cancer counts tended to be high and thus were not smoothed much by any method, while counts of the other cancers were much lower and thus smoothed considerably more (see also Figure 7). Since SANOVA with  $HA_1$ ,  $HA_2$  and estimated  $H_A^{(+)}$  gave very similar results, only those for  $HA_1$  are shown. Results for MCAR0.002 are similar to those for MCAR1, so they are omitted. As expected, MCAR200 shows the least shrinkage among the three MCARs and gives some odd  $\mu_{ij}/E_{ij}$ . To compare models, we calculated the Deviance Information Criterion (DIC; Spiegelhalter et al., 2002). To define DIC, define the deviance  $D(\theta) = -2 \log f(\mathbf{y}|\theta) + 2 \log h(\mathbf{y})$ , where  $\theta$  is the parameter vector in the likelihood and  $h(\mathbf{y})$  is a function of the data. Since  $h$  does not affect model comparison, we set  $\log h(\mathbf{y})$  to 0. Let  $\bar{\theta}$  be the posterior mean of  $\theta$  and  $\bar{D}$  the posterior expectation of  $D(\theta)$ . Then define  $p_D = \overline{D(\theta)} - D(\bar{\theta})$  to be a measure of model complexity and define  $DIC = \bar{D} + p_D$ . Table 4 shows  $\bar{D}$ ,  $p_D$  and  $DIC$  for nine analyses, SANOVA with 3 different  $H_A^{(+)}$ , MCAR

with 3 different priors for  $\Omega$ , and 3 fits of univariate CAR models to the individual diseases, discussed below. Considering  $\overline{D}$ , the three SANOVAs and MCAR1 are similar; Figures 4 to 6 show the fits are indeed similar. Figure 7 reinforces this point, showing that MCAR1 and SANOVA with  $HA_1$  induce similar smoothing for the three cancers. SANOVA with  $H_A^{(+)}$  estimated from MCAR has the smallest  $\overline{D}$  (1458), though its model complexity penalty ( $p_D = 103$ ) is higher than MCAR0.002's ( $p_D = 79$ ). Despite having the second worst fit ( $\overline{D}$ ), MCAR0.002 has the best DIC, and the three SANOVAs have DICs much closer to MCAR0.002's than to the other MCARs'. Generally, all SANOVA models have similar  $\overline{D}$  ( $\approx 1460$ ) and  $DIC$  ( $\approx 1562$ ), while MCAR results are sensitive to  $\Omega$ 's prior, consistent with the simulation experiment. For comparison, we fit separate univariate CAR models to the three diseases considering three different priors for the smoothing precision,  $\tau \sim \text{Gamma}(a, a)$  for  $a = 0.001, 1, \text{ and } 1000$ . For each prior, we added up  $\overline{D}$ ,  $p_D$  and  $DIC$  for three diseases (see Table 4). With  $a = 0.001$  and  $1$ , we obtained  $\overline{D}$ 's (1461 and 1453 respectively) competitive with SANOVA, MCAR0.002 and MCAR1 but with considerably greater complexity penalties (141 and 149 respectively) and thus DICs slightly larger than 1600. For  $a = 1000$ , we obtained an even lower  $\overline{D}$  (1432) but an increased penalty (180) resulted in a poorer  $DIC$  score. Figure 7 shows fitted values for CAR1, which were smoothed like MCAR1 and SANOVA for lung and esophagus cancers but smoothed rather more for larynx cancer. Overall, these results reflect some gain in performance from accounting for the space-cancer interactions/associations.

To further examine the smoothing under SANOVA, Figure 8 shows sep-

arate maps for the county main effect and interactions from the SANOVA fit with  $HA_1$ . The upper left plot is the cancer main effect, the mean of the three cancers; the lower left plot is the comparison of lung versus average of larynx and esophagus; the lower right plot is the comparison of larynx versus esophagus. All values are on the same scale as  $y_{ij}/E_{ij}$  in Figures 4 to 6 and use the same legend. The two interaction contrasts are smoothed much more than the county main effect, agreeing with previous research that larynx and esophagus cancer are closely related spatially (Baron et al 1993). To see whether the interactions are necessary, we fit a SANOVA model (using  $HA_1$ ) without the interactions. As expected, model complexity decreased ( $p_D = 77$ ), while  $\bar{D}$  increased slightly, so DIC became 1558, a bit better than SANOVA with interactions. Now consider the posterior of the MCAR's precision matrix  $\Omega$ . The posterior mean of  $\Omega$  is much larger for MCAR0.002 than MCAR200; the diagonal elements are larger by 4 to 5 orders of magnitude. This may explain the poor coverage for MCAR0.002 in the simulation. Further, consider the correlation matrix arising from the inverse of  $\Omega$ 's posterior mean. As the diagonals of  $R$  change from 0.002 to 200, the correlation between any two cancers decreases and the complexity penalty  $p_D$  increases. By comparison, the three SANOVAs have similar model fits and complexity penalties, leading to similar DICs. So again, in this sense SANOVA shows greater stability.

**5. Discussion and future work.** We used SANOVA to do spatial smoothing and compared it with the much more complex MCAR model. For the cases considered here, we found SANOVA with spatial smoothing to be an excellent competitor to MCAR. It yielded essentially indistinguishable

inference, while being easier to fit and interpret. In the SANOVA model,  $H_A^{(+)}$  is assumed known. For most of the SANOVA models considered,  $H_A^{(+)}$ 's first column was fixed to represent the average over diseases, while other columns were orthogonal to the first column. Alternatively,  $H_A^{(+)}$  could be treated as unknown and estimated as part of the analysis. With this extension, SANOVA with spatial effects is a re-parameterization of the MCAR model and gains the MCAR model's flexibility at the price of increased complexity. This extension would be non-trivial, involving sampling from the space of orthogonal matrices while avoiding identification problems arising from, e.g., permuting columns of  $H_A^{(+)}$ . Other covariates can be added to a spatial SANOVA. Although (10) is a saturated model, spatial smoothing "leaves room" for other covariates. Such models would suffer from collinearity of the CAR random effects and the fixed effects, as discussed by Reich et al. (2006), who gave a variant analysis that avoids the collinearity. For datasets with spatial and temporal aspects, e.g., the 11 years in the Minnesota 3-cancer data, interest may lie in the counts' spatial pattern and in their changes over time. By adding a time effect, SANOVA can be extended to a spatiotemporal model. Besides spatial and temporal main effects, their interactions can also be included and smoothed. There are many modeling choices; the simplest model is an additive model without space-time interactions, where the spatial effect has a CAR model and the time effect a random walk, which is a simple CAR. But many other choices are possible. We have examined intrinsic CAR models, where  $Q_{ij} = -1$  if region  $i$  and region  $j$  are connected. SANOVA with spatial smoothing could be extended to more general CAR models. Banerjee et al. (2004) replaced  $Q$  with the

matrix  $D_w - \rho W$ , where  $D_w$  is diagonal with the same diagonal as  $Q$  and  $W_{ij} = 1$  if region  $i$  is connected with region  $j$ , otherwise  $W_{ij} = 0$ . Setting  $\rho = 1$  gives the intrinsic CAR model considered in this paper. For known  $\rho$ , the SANOVA model described here is easily extended by replacing  $Q$  in Section 2 with  $D_w - \rho W$ . However, for unknown  $\rho$ , our method cannot be adjusted so easily, because updating  $\rho$  in the MCMC would force  $V$  and the design matrix to be updated as well, but this would change the definition of the parameter  $\Theta$ . Therefore, a different approach is needed for unknown  $\rho$ . A different extension of SANOVA would be to survival models for areal spatial data (e.g., Li & Ryan, 2002; Banerjee, Wall & Carlin, 2003; Diva, Dey and Banerjee, 2008). If the regions are considered strata, then random effects corresponding to nearby regions might be similar. In other words, we can embed the SANOVA structure in a spatial frailty model. For example, the Cox model with SANOVA structure for subject  $j$  in stratum  $i$  is

$$(18) \quad h(t_{ij}, X_{ij}) = h_0(t_{ij}) \exp(X_{ij}\beta),$$

where  $X$  is the design matrix, which may include a spatial effect, a temporal effect, their interactions and other covariates. Banerjee et al. (2004) noted that in the CAR model, considering both spatial and non-spatial frailties, the frailties are identified only because of the prior, so the choice of priors for precisions is very important. Besides the above extensions, HCSC introduced tools for normal SANOVA models that can be extended to non-normal SANOVA models. For example, HCSC defined the degrees of freedom in a fitted model as a function of the smoothing precisions. This can be used as a measure of the fit's complexity, or a prior can be placed on the degrees of freedom as a way of inducing a prior on the unknowns in the variance

structure. The latter is under development and will be presented soon.

**Acknowledgements.** The authors thank the referees, the Associate Editor and the Editor for valuable comments and suggestions. The third author also acknowledges the support of NIH grant 1-R01-CA95995.

## SUPPLEMENTARY MATERIAL

### Appendices, data and code

(doi: <http://lib.stat.cmu.edu/aoas/???/???; .pdf>). Our supplementary material includes four sections as appendices. In Appendix A we present a derivation of the precision matrix of (11). Details of our MCMC algorithms can be found in Appendix B. Appendix C discusses the mean transformation for the Poisson case while Appendix D discusses the estimation of the  $H_A^{(+)}$  from MCAR1. In addition we provide a compressed folder containing the data set for our 3-cancer Minnesota example as well as an R code example to implement the SANOVA models.

### 6. References.

- Banerjee S, Carlin BP, Gelfand AE (2004). *Hierarchical Modeling and Analysis for Spatial Data*. Boca Raton, FL: Chapman & Hall/CRC Press.
- Banerjee S, Wall MM, Carlin BP (2003). Frailty modeling for spatially correlated survival data, with application to infant mortality in Minnesota. *Biostatistics*, 4:123-142.
- Baron AE, Franceschi S, Barra S, Talamini R, La Vecchia C (1993). Comparison of the joint effect of alcohol and smoking on the risk of cancer across sites in the upper aerodigestive tract. *Cancer Epidemiology Biomarkers and Prevention*, 2:519-523.

- Besag J (1974). Spatial interaction and the statistical analysis of lattice systems (with discussion). *J. Roy. Stat. Soc., Ser. B*, 36:192-236.
- Besag, J, Green, P, Higdon, D, Mengersen, K (1995). Bayesian computation and stochastic systems (with discussion). *Statist. Science* 10:3-66.
- Besag, J, York, JC, and Mollié, A (1991). Bayesian image restoration, with two applications in spatial statistics (with discussion). *Annals of the Institute of Statistical Mathematics*, 43:1-59.
- Carlin, BP and Banerjee, S (2003). Hierarchical multivariate CAR models for spatio-temporally correlated survival data. In *Bayesian Statistics 7*, eds. J.M. Bernardo et al., Oxford: Oxford University press, pp.45-64.
- Elliott P, Wakefield JC, Best NG, Briggs DJ, eds. (2000). *Spatial Epidemiology: Methods and Applications*. Oxford: Oxford University Press.
- Gelfand AE, Vounatsou P (2003). Proper multivariate conditional autoregressive models for spatial data analysis. *Biostatistics*, 4:11-25.
- Haran M, Hodges JS, Carlin BP (2002). Accelerating computation in Markov random field models for spatial data via structured MCMC. *J. Comp. Graph. Stat.*, 12:249-264.
- He Y, Hodges JS, Carlin BP (2007). Re-considering the variance parameterization in multiple precision models. *Bayes. Anal.*, 2:1-28.
- Hodges JS (1998). Some algebra and geometry for hierarchical models. *J. Roy. Stat. Soc., Ser. B*, 60:497-536.
- Hodges JS, Sargent DJ (2001). Counting degrees of freedom in hierarchical and other richly-parameterised models. *Biometrika*, 88:367-379.
- Hodges JS, Carlin BP, Fan Q (2003). On the precision of the conditionally autoregressive prior in spatial models. *Biometrics*, 59:317-322.

- Hodges JS, Cui Y, Sargent DJ, Carlin BP (2007). Smoothing balanced single-error-term analysis of variance. *Technometrics*, 49:12-25.
- Jin X, Carlin BP, Banerjee S (2005) Generalized hierarchical multivariate CAR models for areal data. *Biometrics*, 61:950-961.
- Jin X, Banerjee S, Carlin BP (2007). Order-free coregionalized lattice models with application to multiple disease mapping. *J. Roy. Stat. Soc., Ser. B*, 69:817-838.
- Kim H, Sun D, Tsutakawa RK (2001). A bivariate Bayes method for improving the estimates of mortality rates with a twofold conditional autoregressive model. *J. Amer. Stat. Assn.*, 96:1506-1521.
- Lawson AB, Biggeri AB, Bohning D, Lesaffre E, Viel JF, Bertollini R (1999). *Disease Mapping and Risk Assessment for Public Health*, New York: John Wiley.
- Lee Y, Nelder JA (1996). Hierarchical generalized linear models (with discussion). *J. Roy. Stat. Soc., Ser. B*, 58:619-673.
- Li Y, Ryan L (2002). Modeling spatial survival data using semi-parametric frailty models. *Biometrics*, 58:287-297.
- Lichstein JW, Simons TR, Shriener SA, Franzreb KE (2002). Spatial autocorrelation and autoregressive models in ecology. *Ecological Monographs*, 72:445-463.
- Lu H, Hodges JS, Carlin BP (2004). Measuring the complexity of generalized linear hierarchical models. *Can. J. Stat.*, 19:69-87.
- Mardia KV (1988). Multi-dimensional multivariate Gaussian Markov random fields with application to image processing. *J. Multivar. Anal.*, 24:265-284.

- Ramsay, T, Burnett, R, and Krewski, D (2003). Exploring bias in a generalized additive model for spatial air pollution data. *Environmental Health Perspectives*, 111:1283-1288.
- Reich BJ, Hodges JS, Zadnik V (2006). Effects of residual smoothing on the posterior of the fixed effects in disease-mapping models. *Biometrics*, 62:1197-1206.
- Rue H, Held L (2005). *Gaussian Markov Random Fields: Theory and Applications*. Boca Raton: Chapman and Hall/CRC.
- Sain SR, Cressie N (2002). Multivariate lattice models for spatial environmental data. In *Proc. A.S.A. Section on Statistics and the Environment*. Alexandria, VA: American Statistical Association, pp. 2820-2825.
- Sargent DJ, Hodges JS, Carlin BP (2000). Structured Markov chain Monte Carlo. *J. Comp. Graph. Stat.*, 9:217-234.
- Turechek, WW and Madden, LV (2002). A generalized linear modeling approach for characterizing disease incidence in spatial hierarchy. *Phytopathology*, 93:458-466.
- Wakefield J (2007). Disease mapping and spatial regression with count data. *Biostatistics*, 8:158-183.
- Wall MM (2004). A close look at the spatial structure implied by the CAR and SAR models. *J. Stat. Plan. Inf.* 121:311-324.
- Waller LA, Gotway CA (2004). *Applied Spatial Statistics for Public Health Data*. New York: Wiley.
- Zhang, Y., Hodges, J.S. and Banerjee, S. (2009). Supplement to “Smoothed ANOVA with spatial effects as a competitor to MCAR in multivariate

spatial smoothing.” DOI:????

Error distribution	$\eta_0$	$(\tau_0/\eta_0, \tau_1/\eta_0, \tau_2/\eta_0)   (\tau_0, \tau_1, \tau_2)$	Data Name
Normal	1	(100,100,0.1)	Data1
	1	(0.1,100,0.1)	Data2
	10	(100,100,0.1)	Data3
	10	(0.1,100,0.1)	Data4
Poisson	NA	(100,100,0.1)	Data5
	NA	(0.1,100,0.1)	Data6

TABLE 1

*Experimental conditions in the simulation experiments*

procedure	prior
SANOVA with correct $H_A^{(+)}$	$\eta_0, \tau_j \sim \Gamma(0.1, 0.1)$ for $j = 0, 1, 2$
SANOVA with incorrect $H_A^{(+)}$	$\eta_0, \tau_j \sim \Gamma(0.1, 0.1)$ for $j = 0, 1, 2$
variant SANOVA with $H_{AM}$	$\eta_0, \tau_j \sim \Gamma(0.1, 0.1)$ for $j = 0, 1, 2$
MCAR	$\Omega \sim Wishart(R, 3), R = 0.002I_3$
MCAR	$\Omega \sim Wishart(R, 3), R = I_3$
MCAR	$\Omega \sim Wishart(R, 3), R = 200I_3$

TABLE 2

*The six statistical methods used in the simulation experiment*

model	normal-error model				Poisson-error model	
	Data1	Data2	Data3	Data4	Data5	Data6
SANOVA with $HA_1$	0.34	0.60	0.04	0.06	0.02	0.04
SANOVA with $HA_2$	0.47	0.84	0.05	0.07	0.02	0.14
SANOVA with $HA_{AM}$	0.48	0.74	0.05	0.06	0.03	0.11
MCAR with $R_{ii} = 0.002$	0.66	1.88	0.04	0.13	0.02	0.04
MCAR with $R_{ii} = 1$	0.36	0.84	0.04	0.06	0.02	0.06
MCAR with $R_{ii} = 200$	0.93	0.92	0.09	0.09	0.24	0.36

TABLE 3

*AMSE for simulated normal and Poisson data*

Model	$\bar{D}$	$p_D$	DIC
SANOVA with $H_{A1}$	1461	103	1564
SANOVA with $H_{A2}$	1463	102	1565
SANOVA with $H_A$ estimated from MCAR1	1458	103	1561
MCAR0.002	1476	79	1555
MCAR1	1459	132	1591
MCAR200	1559	356	1915
CAR0.001	1461	141	1602
CAR1	1453	149	1602
CAR1000	1432	180	1612

TABLE 4  
Model comparison using DIC

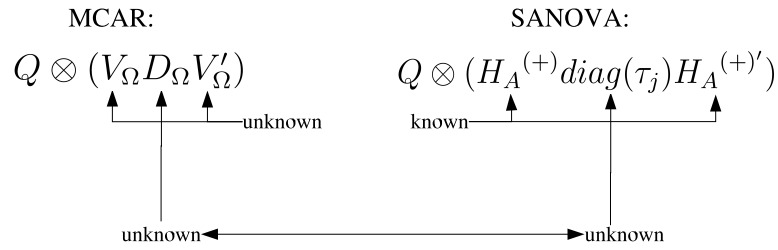


Fig 1: Comparing prior precision matrices for  $\phi$  in MCAR and SANOVA.

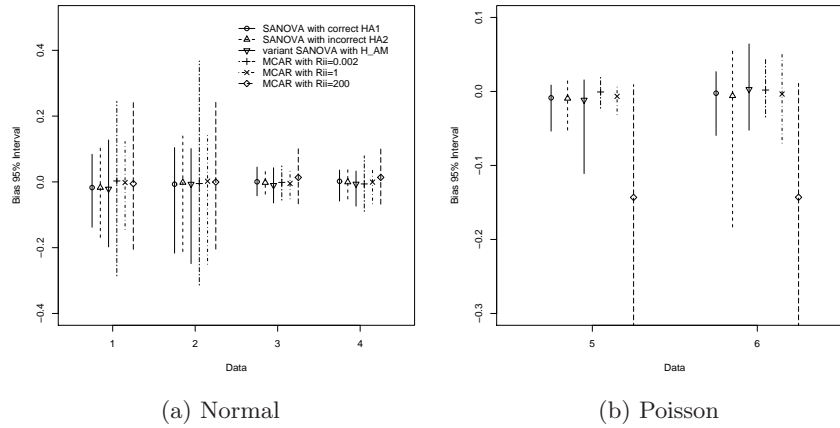


Fig 2: MBIAS for simulated normal and Poisson data

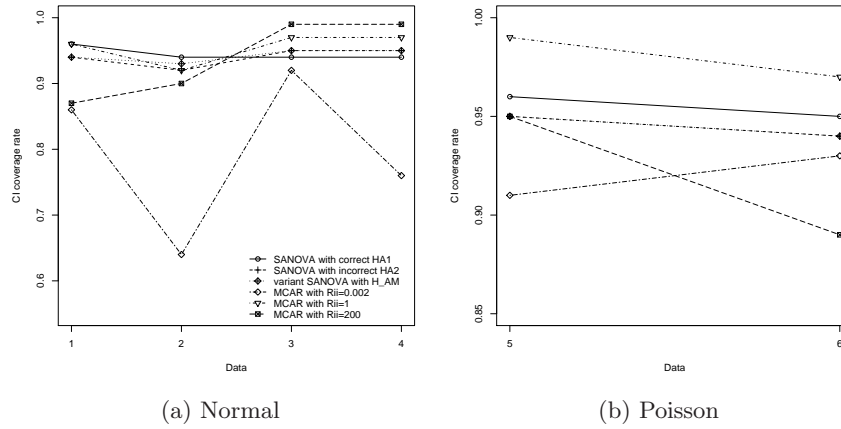


Fig 3: PI rate for simulated normal and Poisson data

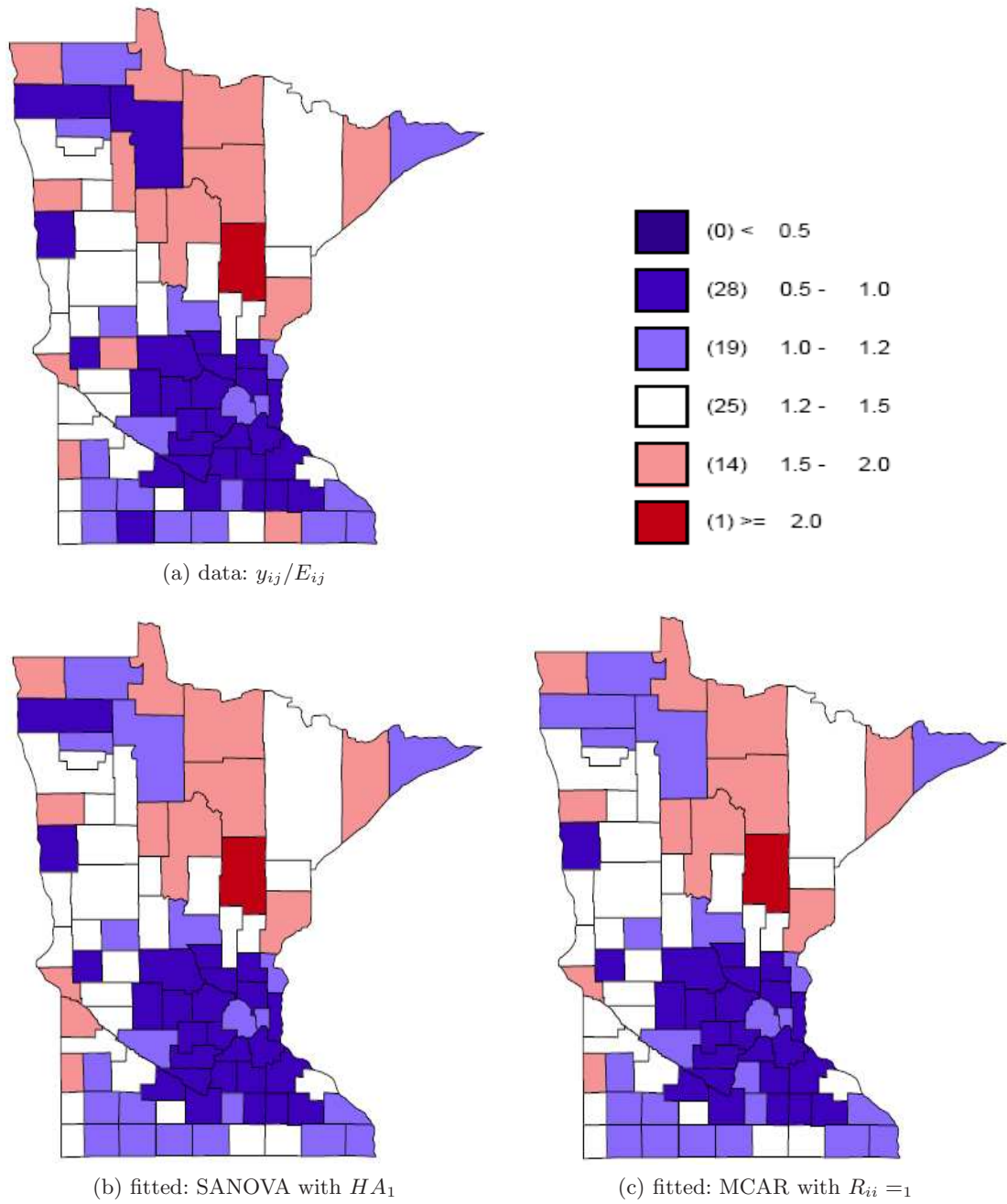


Fig 4: Lung cancer data and fitted values

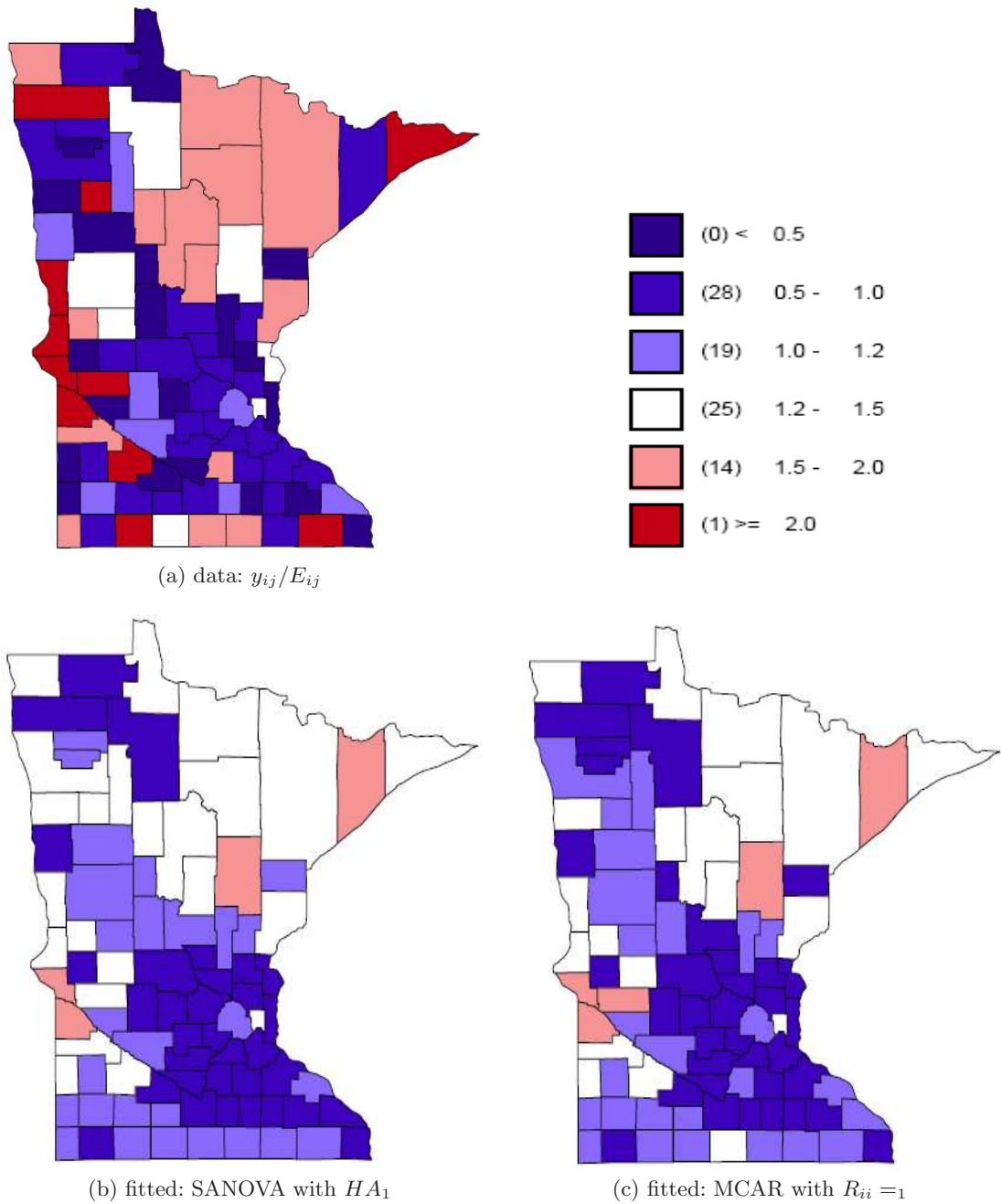


Fig 5: Larynx cancer data and fitted values

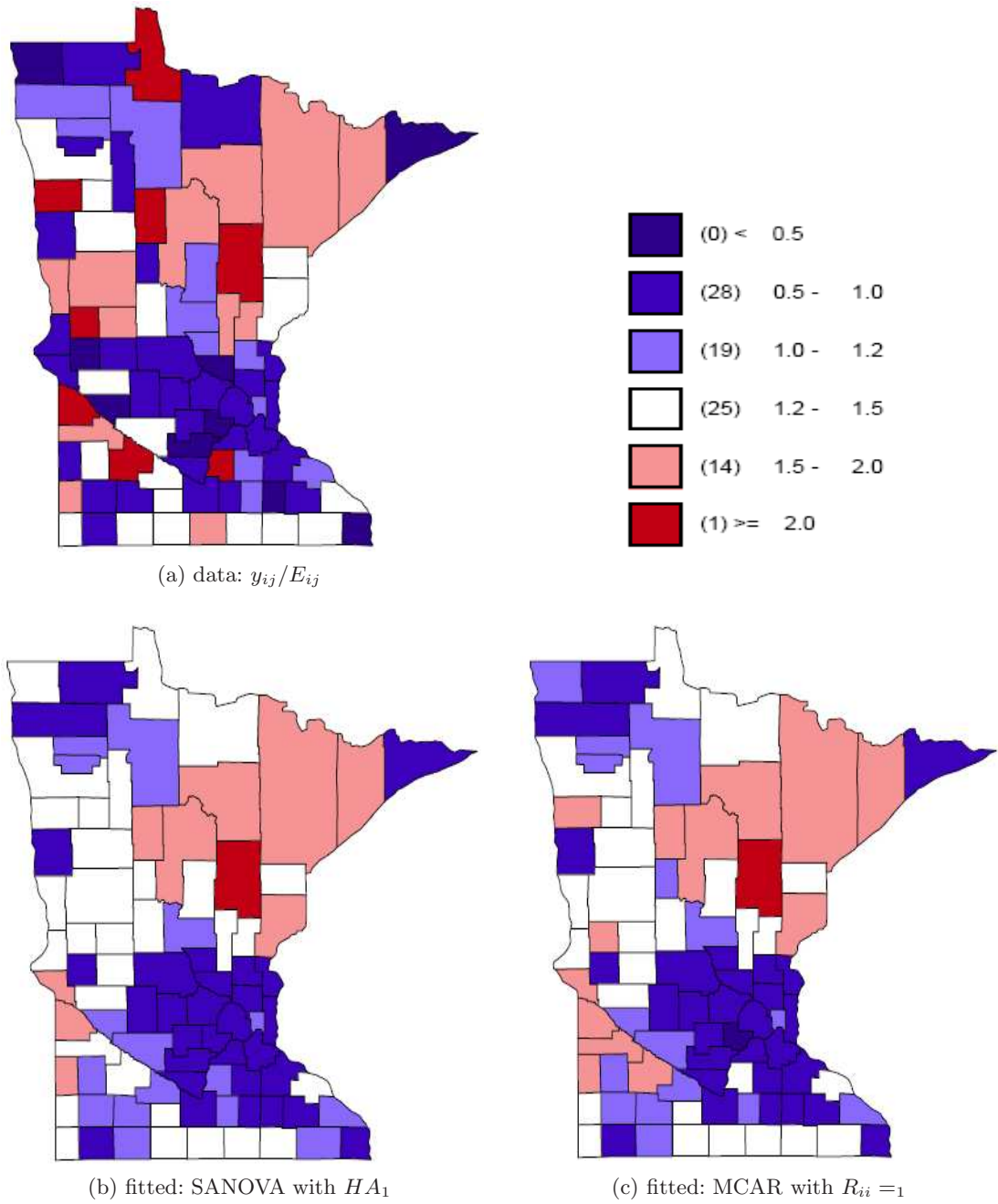


Fig 6: Esophagus cancer data and fitted values

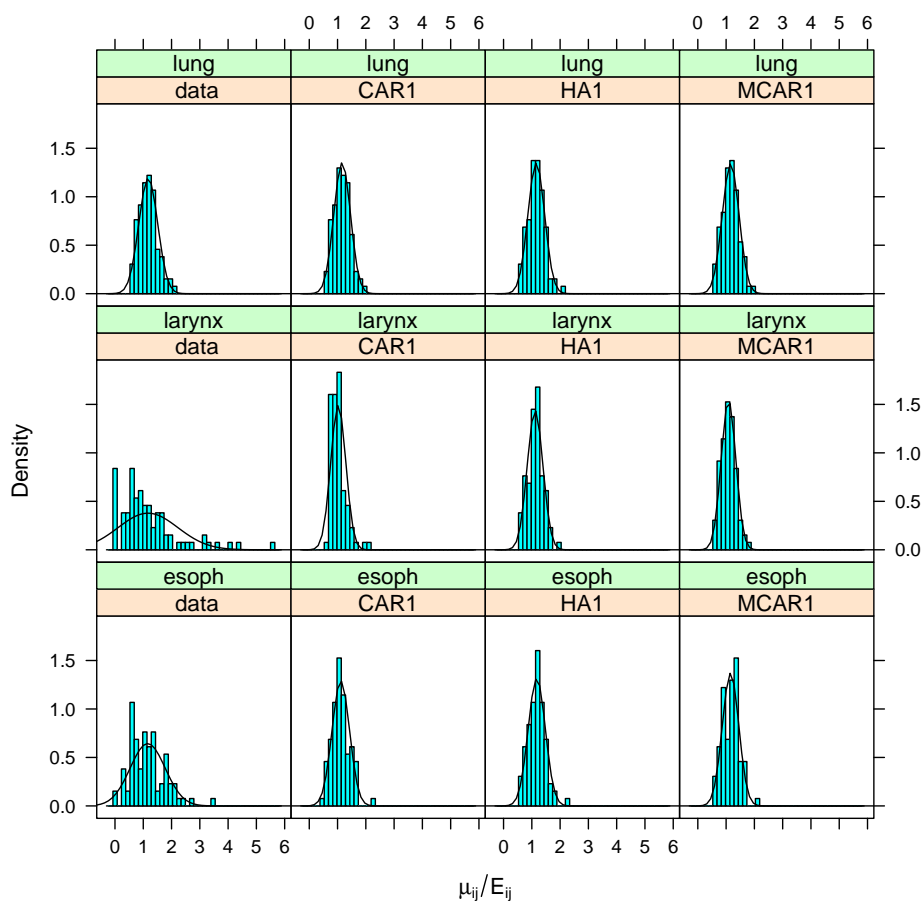
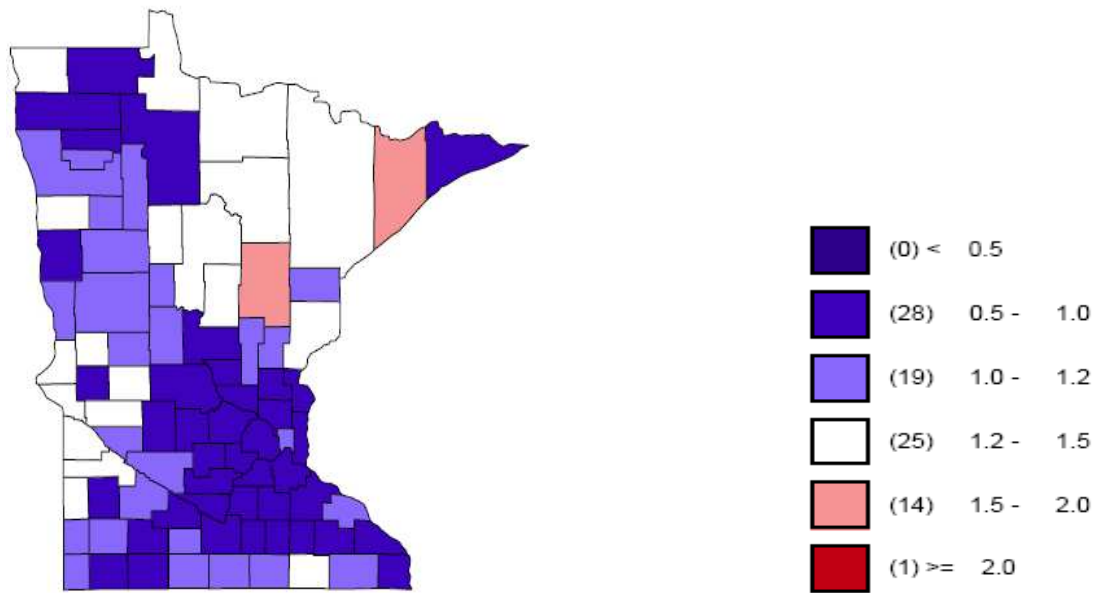
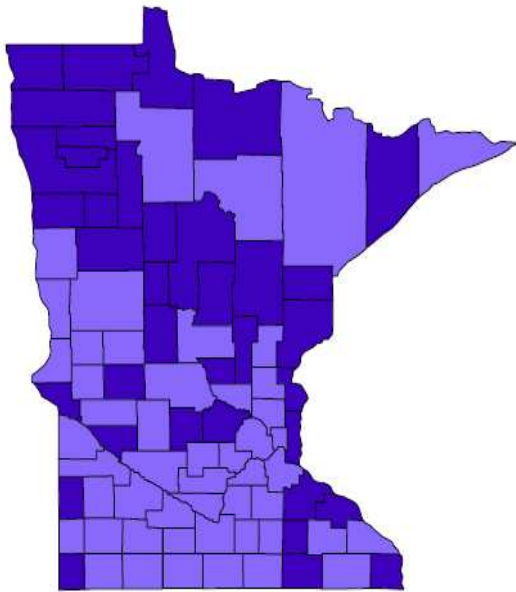


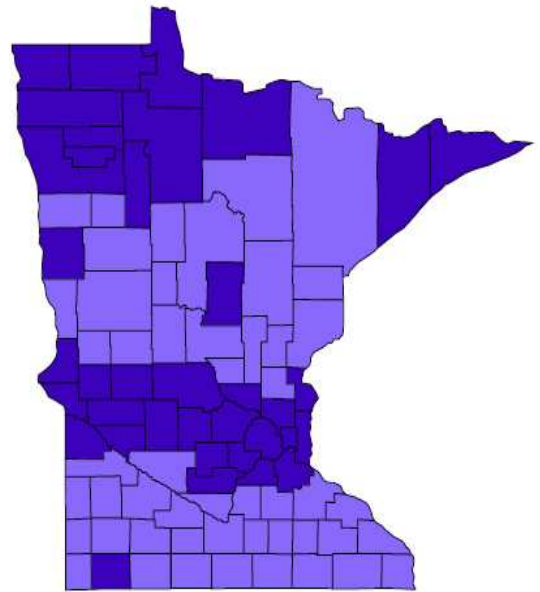
Fig 7: Comparing data and fitted values for each cancer. The “Data” panel shows the density for  $y_{ij}/E_{ij}$ , while the other three panels show the posterior median of  $\mu_{ij}/E_{ij}$  for univariate CAR, SANOVA and MCAR;



(a)



(b)



(c)

Fig 8: SANOVA with  $HA_1$ : (a) county main effect; (b) cancer  $\times$  county interaction 1 for larynx; (c) cancer  $\times$  county interaction 2 for esophagus.